DOI: 10.1002/ejic.200900303

New Helical Zinc Complexes with Schiff Base Derivatives of β-Diketonates or β-Keto Esters and Ethylenediamine

Oxana Kotova,*[a] Sergey Semenov,[a] Svetlana Eliseeva,[a] Sergey Troyanov,[a] Konstantin Lyssenko,[b] and Natalia Kuzmina[a]

Keywords: Zinc / Schiff bases / Helical structures / Chelates / Luminescence

The tetradentate Schiff bases H_2L = H_2AC [*N*,*N*′-ethylene-bis(4-iminopentan-2-one)], H_2MAL1 [*N*,*N*′-ethylene-bis-(methyl-3-iminobutanoate)], and H_2MAL2 [*N*,*N*′-ethylene-bis(*tert*-butyl-3-iminobutanoate)] were found to possess sufficient flexibility and were tailored to self assemble with zinc ions to form neutral bimetallic helicates with the overall composition Zn_2L_2. In solution for all ligands, an equilibrium between the tautomeric forms exists, which was confirmed by IR and NMR spectroscopy. X-ray single-crystal analysis performed for H_2MAL1 (**1**) and H_2MAL2 (**2**) reveals that they have similar geometrical parameters and crystallize in a *trans* conformation. In the crystal structures of the zinc complexes $[Zn_2(AC)_2]\cdot C_6H_6$ (**3**), $[Zn_2(MAL1)_2]\cdot 0.5C_7H_8$ (**4**), and $[Zn_2(MAL2)_2]\cdot C_7H_8$ (**5**), the Schiff base ligands are helically wrapped around the two four-coordinate metal ions, which leads to an idealized D_2 symmetry. The coordination polyhedron around the Zn ions in **3**–**5** can be described as a tetrahedral geometry comprising two O- and two N-donor atoms of the Schiff base ligands. The intramolecular separation Zn···Zn varies from 3.465 to 3.628 Å. The total length of the helix is 5.85, 5.84, and 6.01 Å for structures **3**, **4**, and **5**, respectively, while the helical pitch values are in the range 7.8–9.2 Å. Both the ligands H_2L and the zinc helicates are thermally stable up to ≈150–160 °C, as shown by thermogravimetric analysis under a nitrogen atmosphere. The formation of the zinc complexes in solution is confirmed by spectrophotometric titrations, along with ESI-MS, and has almost no effect on the absorption spectra of H_2L. The Schiff bases and the Zn_2L_2 complexes display broad-band, blue emission in the range 350–600 nm under a 337-nm excitation at 77 K. Finally, the impact of electronic effects of the Schiff base substituents on the structure of the Zn complexes, especially on bond lengths within the chelate rings, and the absorption and photoluminescence spectra, are discussed.

Introduction

Zinc complexes with Schiff bases have found different applications in various fields of materials science.[1] For example, they are known to be strong fluorescent emitters,[2] the photophysical characteristics of which can easily be tuned by slightly modifying the substituents on the organic ligands.[3] These compounds can be used as active layers in organic light-emitting diodes (OLEDs),[4] as metal containing gels and nanofibers for different biological applications,[5] and as fluorescent detectors of nanoaromatic and explosive mimics.[6]

Herein we investigate zinc complexes with tetradentate Schiff bases. The stereochemistry of zinc in such systems began to be investigated a long time ago. The study of Batley and Graddon in 1967 showed that the coordination number of zinc in complexes with tetradentate ligands is determined solely by the steric properties of the latter. When a Schiff base provides a tetrahedral environment around the zinc ion, no further coordination (for example, by solvent molecules) occurs. Conversely, when such an environment cannot be obtained, additional coordination takes place and a 5-coordination pattern is observed.[7] For instance, in zinc complexes with tetradentate *N*,*N*′-ethylene-bis(salicylideneimine) (H_2salen), the metallic center has a square-pyramidal coordination polyhedron formed by four donor atoms of $salen^{2-}$ and one water molecule, as a consequence of the inability of the Schiff base to provide the required tetrahedral environment around the metal ion.[8] In 2002, Reglinski et al.[9a] and later Knapp[6] and Kleij[1b–1d,1g] analyzed the structures of zinc complexes with H_2salen derivatives and showed that in these systems the zinc atom preferably adopts a five-coordinate square-pyramidal environment. However, in spite of this, Muzukami and Kanesato [9b] demonstrated in 2003 that the tendency of zinc to favor five coordination in salen-type complexes can be hindered by the introduction of *tert*-butyl groups in positions adjacent to the coordinating hydroxyl groups, namely the 3 and 3′ positions. A tetrahedral coordination environment, in this case, was achieved by self-as-

[a] Department of Chemistry, Lomonosov Moscow State University,
Leninskie Gory, 119991 Moscow, Russia
Fax: +7-495-939-09-98
E-mail: kotova@inorg.chem.msu.ru
[b] A. N. Nesmeyanov Institute of Organoelement Compounds, Russian Academy of Sciences,
28 Vavilov Street, 119991 Moscow, Russia
Supporting information for this article is available on the WWW under http://dx.doi.org/10.1002/ejic.200900303.

sembly, and the first helical Zn(salen) derivative with interesting optical properties was obtained.[9b,9c] Several other analogous helical complexes have been described recently, but examples of Zn Schiff base helicates remain quite rare.[10]

Here, tetradentate Schiff base (H_2L) derivatives of 2,4-acetylacetone (H_2AC), methylacetoacetate (H_2MAL1) or *tert*-butylacetoacetate (H_2MAL2), and ethylenediamine (Figure 1) were chosen in order to exploit the tendency of the zinc ion to achieve a square-pyramidal coordination.

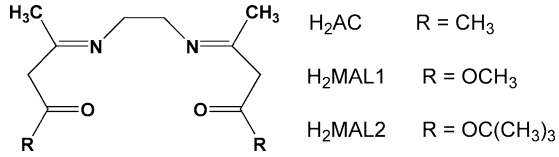

Figure 1. Structures of H_2L: H_2AC, H_2MAL1, H_2MAL2.

The interactions between diethylzinc and H_2L yields dinuclear, helical species, Zn_2L_2. The Schiff bases and zinc complexes were structurally characterized, and their thermal and optical properties were investigated. The influence of the nature of the Schiff bases, namely the effect of substituents R (Figure 1), on the synthesis of the corresponding Zn complexes, on their crystal structure, as well as on their optical properties was evaluated and a comparison with H_2salen derivatives was drawn.

Results and Discussion

Synthesis and Characterization

In general, five different synthetic routes can be considered for the preparation of Schiff base metal complexes.[11] Each of them has its own advantages and disadvantages, and the choice of method mostly depends on the nature of both the metal ion and the Schiff base. The simplest and, thus most common, synthetic approach is reaction between metal acetate and the relevant Schiff base. This reaction is insensitive to moisture and air, and the main by-product, acetic acid, can easily be removed from the Schiff base complexes by thermal treatment at ≈40–80 °C under reduced pressure. However, in some cases, acetic acid is not the only contaminant as an admixture of the initial reagents may also be present. The removal of those initial compounds becomes particularly difficult for highly soluble, thermally unstable, or nonvolatile Schiff base complexes.[12,13] The second quite easily performed synthetic route consists of reacting Schiff bases with metal alkoxides. However, the presence of trace amounts of water in the reaction mixture often results in complexes contaminated with μ-oxo species. Metal amides (third route) or alkyls (forth route) can also be used as initial reagents; the only by-products are volatile amines or alkanes.[11,14] Metal complexes with Schiff base derivatives of salicylic aldehyde can be also obtained by a two-step reaction including the deprotonation of the Schiff base with sodium- or potassium hydride followed by reaction with a metal halide (fifth route). The last three synthetic routes allow the obtainment of pure final products with high yields, but they are more complicated and have to be conducted under an inert atmosphere because of the high moisture sensitivity and reactivity of the initial reagents.

In this work, we tried to synthesize zinc complexes by the reaction between zinc acetate and the relevant Schiff base. However, the final complexes were contaminated with acetic acid and the initial compounds. Purification of the obtained product by recrystallization or thermal treatment/sublimation was not effective because of the high solubility of the initial reagents and of the zinc Schiff base complex, in addition to low thermal stability and volatility of the latter. Thus, we turned to the following high-yield synthetic route [Equation (1)].[14]

$$Zn(Et)_2 + H_2L \xrightarrow[-C_2H_6]{} 0.5\,Zn_2L_2 \quad (1)$$

This reaction leads to the formation of the expected products with the general composition Zn_2L_2 (H_2L = H_2AC, H_2MAL1, H_2MAL2) in a good yield (86–92%) as a result of the high reactivity of $Zn(Et)_2$ and the strong acidic character of the Schiff base protons. Ethane is the only by-product for this reaction, and it is easily removed from the reaction mixture.

The infrared spectra of the zinc Schiff base complexes display the typical ν(C=C) + ν(C=N) + ν(C=O) and ν(C–H) vibrations in the regions 1655–1580 and 3100–2800 cm^{-1}, respectively. In addition, for $Zn_2(MAL1)_2$ and $Zn_2(MAL2)_2$, ν(O–CH_3) and ν(O–C{CH_3}$_3$) bands are observed in the ranges 1100–1050 and 850–810 cm^{-1}, respectively. It is worth noting that in the IR spectra of the initial Schiff bases, the ν(N–H) vibrations are present in the region 3300–3100 cm^{-1}, along with ν(C–O–H) at 1200–1000 cm^{-1}. This observation, together with the singlet signals located at δ ≈ 10.88–8.60 ppm in the NMR spectra, confirms the existence of an equilibrium between the tautomeric forms for all H_2L ligands studied (Figure 2).

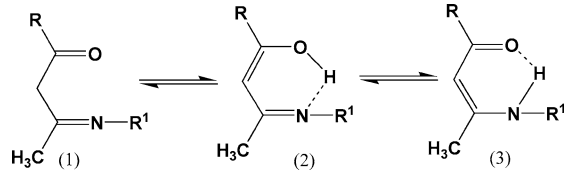

Figure 2. Equilibrium between the tautomeric forms.

The most intense peaks in the ESI-MS spectra of the corresponding Zn_2L_2 complexes can be attributed to the monometallic ions $[Zn(AC) + H^+]^+$ (m/z = 286.9, 80%), $[Zn(MAL1) + H^+]^+$ (319.0, 100%) and $[Zn(MAL2) + H^+]^+$ (403.0, 50%), which thereby gives additional confirmation on the formation of Zn complexes in solution.

Molecular Structures

Schiff Bases

The covalent bond lengths and angles in H_2MAL1 (R = –OCH_3) and H_2MAL2 [R = –$OC(CH_3)_3$] (Figure 3) are rather similar to those for H_2AC.[15] Both molecules crystallize in the keto–enamine form stabilized by intramolecular N–H···O bonds. The N···O distance in H_2MAL1 [2.785(5) Å] is longer than that in H_2MAL2 [2.691(6) Å] and H_2AC (2.692 Å). The weakening of the hydrogen bond in H_2MAL1 is caused by the presence of an additional intermolecular hydrogen bond N1–H(1N)···O1 (½ – *x*; –½ + *y*; ½ – *z*) [N1···O1 3.155(5) Å, N1–H(1N)–O1 134°]. Hydrogen-bonding cycles in H_2MAL1, H_2MAL2, and H_2AC are characterized by a *trans* disposition with respect to the central $N(CH_2)_2N$ moiety, while similar Schiff base with R = –OC_2H_5[16] exist in a *cis* conformation. By assuming a flexible central saturated fragment, it is reasonable to conclude that the disposition of H-bonded patterns is mainly governed by crystal-packing effects. Indeed, the torsion angle N–C–C–N in H_2MAL1 and H_2MAL2 is close to 180°, while in the crystals of the Schiff bases with R = –CH_3 (H_2AC) and R = –OC_2H_5, the N–C–C–N fragment is characterized by a *syn*-periplanar conformation (torsion angle N–C–C–N is 64.8–65.3°).

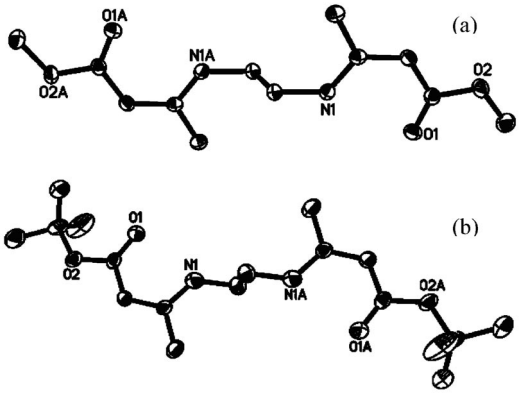

Figure 3. General view of the structures of (a) H_2MAL1 and (b) H_2MAL2.

Zinc Complexes

These structures exemplify the influence of (i) the nature of the Schiff base on the structure of the complexes (Figure 4) and the coordination environment of the metal centers, and (ii) the ligand substituents (R) on the bond length distribution in the chelate cycles (Figure 5, Table 1). The complexes **3**–**5** have a molecular structure consisting of helical Zn_2L_2 blocks with an idealized D_2 symmetry (Figure 4). The packing of the molecules in the crystal structures is governed by Van der Waals interactions and no hydrogen bonding or other specific interactions are observed. The central symmetry of all structures implies that the complexes represent a racemic 1:1 mixture of right- and left-handed isomers. In the studied crystal structures, the zinc ion is surrounded by two oxygen and two nitrogen atoms, each occupying one of the apices of the coordination polyhedron that corresponds to a tetrahedron.

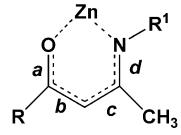

Figure 5. Chelate ring of the bonds in the structural fragment of the Zn complexes.

The formation of such a favorable coordination environment around the Zn atoms becomes possible because of the sufficient flexibility of the chosen Schiff bases. Usually, the rearrangement of Schiff bases is quite difficult because of their rigidity, especially for those containing aromatic bridges,[7] so that mononuclear pentacoordinate structures are mostly observed.

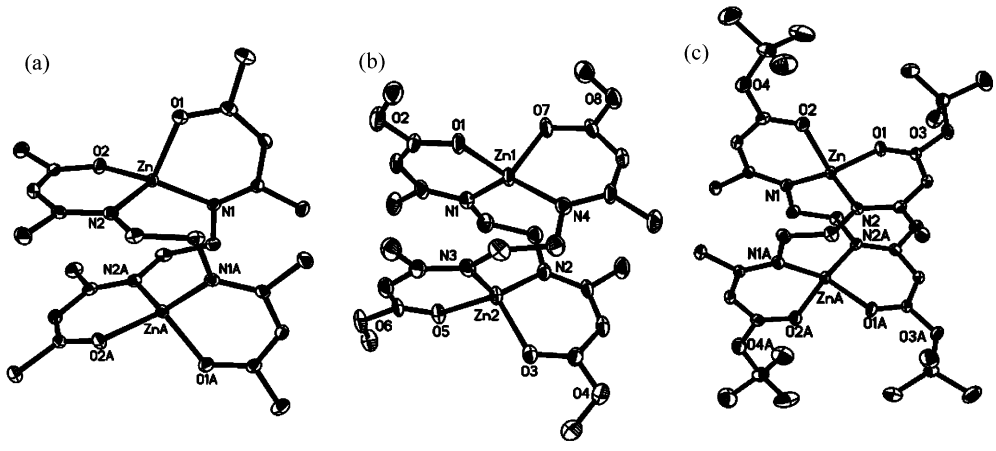

Figure 4. General view of the structures of (a) $[Zn_2(AC)_2]\cdot C_6H_6$, (b) $[Zn_2(MAL1)_2]\cdot 0.5C_7H_8$, and (c) $[Zn_2(MAL2)_2]\cdot C_7H_8$. Solvent molecules are omitted for clarity.

Table 1. Selected bond lengths [Å] and angles [°] in the zinc complexes (the parameters *a*–*d* are depicted in Figure 5).

Parameter	3	4	5
Zn–O	1.960(1); 1.934(1)	1.962(3)–2.007(3)	1.973(2); 2.000(2)
Zn–N	1.983(1); 1.995(1)	1.956(4)–1.985(3)	1.966(2); 1.973(2)
a	1.286(2); 1.288(2)	1.264(5)–1.279(5)	1.273(3); 1.271(3)
b	1.380(2); 1.382(2)	1.376(7)–1.397(6)	1.392(4); 1.401(4)
c	1.427(2); 1.421(2)	1.395(7)–1.425(6)	1.409(3); 1.406(4)
d	1.314(2); 1.316(2)	1.339(5)–1.343(5)	1.337(3); 1.339(3)
e[a]	3.6281(2)	3.465(1); 3.519(1)	3.582(1)
δ[b]	89.5	85.8–89.6	87.3

[a] The distance between the zinc atoms. [b] Dihedral angle between the two planes of the ZnON chelates.

The substitution of the $-CH_3$ group [positive inductive effect (+I)] in $[Zn_2(AC)_2]\cdot C_6H_6$ with $-OCH_3$ or $-OC(CH_3)_3$ groups [negative inductive (–I) and positive mesomeric (+M) effects] when going from $[Zn_2(AC)_2]\cdot C_6H_6$ to $[Zn_2(MAL1)_2]\cdot 0.5C_7H_8$ or $[Zn_2(MAL2)_2]\cdot C_7H_8$ leads to an elongation of the Zn–O bonds and to a contraction of the Zn–N, C–O and C–C bonds (Figure 4, Figure 5, Table 1). The intramolecular separation Zn···Zn varies from 3.465 to 3.628 Å and is generally shorter for $-OCH_3$- and $-OC(CH_3)_3$-substituted derivatives (Table 1). It is worth mentioning that the influence of the substituent R on the distances in the chelate ring is more pronounced for aliphatic Schiff bases than for aromatic ones.[7] The parameters specific to the helical complexes **3**–**5** are summarized in Table 2. The values of the separation between the facial planes [$d(F_i–F_j)$] lie in the range 1.805–2.183 Å. All zinc complexes are characterized by an overall twist around the C_2 axis with almost similar twist angles (ω_{ij} 81–86°) around the metal centers and by the intermetallic domains most typical for double-stranded helices than for triple-helical structures.[17] The total lengths of the helices are 5.85, 5.84, and 6.01 Å for structures **3**, **4**, and **5**, respectively, while the helical pitch [$P_{ij} = d(F_i–F_j)/(\omega_{ij}/360)$] values are in the range 7.8–9.2 Å. The sum of the twist angles is ≈250°, which is approximately 2/3 of a turn per molecule. It can be noted that almost similar helical parameters were observed for Zn helicates with salen-type Schiff bases.[9b,9c]

Table 2. The linear distances $d(F_i–F_j)$, the average twist angles ω_{ij} along the pseudo-C_2 axis in the crystal structures of **3**–**5**, and the helical pitches P_{ij}.

	3			4[a]			5		
	$d(F_i–F_j)$ [Å]	ω_{ij} [°]	P_{ij} [Å]	$d(F_i–F_j)$ [Å]	ω_{ij} [°]	P_{ij} [Å]	$d(F_i–F_j)$ [Å]	ω_{ij} [°]	P_{ij} [Å]
*F*1–*F*2	1.863	81.0	8.3	1.805	83.5	7.8	1.921	80.5	8.6
*F*2–*F*3	2.124	86.0	8.9	2.183	85.0	9.2	2.170	86.0	9.1
*F*3–*F*4	1.863	81.0	8.3	1.848	82.5	8.1	1.921	80.5	8.6

[a] An average value for the two crystallographically independent molecules are presented.

Thermal Analysis

In order to use the complexes as emissive materials it is important to investigate their thermal stability.[18–20] This characteristic can be estimated from the thermal analysis data and, most often, it refers to the temperature at which weight loss begins (T_b). Thus, the thermal behavior of the Schiff bases and their zinc complexes was examined by means of thermogravimetric analysis under a nitrogen atmosphere (Figure 6, Table S1). The total weight loss for ligands H_2L (≈100%) corresponds to the sublimation along with thermal decomposition, while this value for the zinc complexes is somewhat lower (≈80–85%) and can be attributed to decomposition into zinc oxide. The temperature at which weight loss begins was estimated to be ≈150–160 °C for both the Schiff bases and the Zn complexes, which therefore indicates that there is no improvement in the thermal stability when going from H_2L to Zn_2L_2.

Optical Properties

Absorption Spectra

The absorption spectra of H_2L and Zn_2L_2 were investigated in methanol solutions and in the solid state and are very similar and feature the main electronic transitions characteristic of this type of compounds (Figure 7).

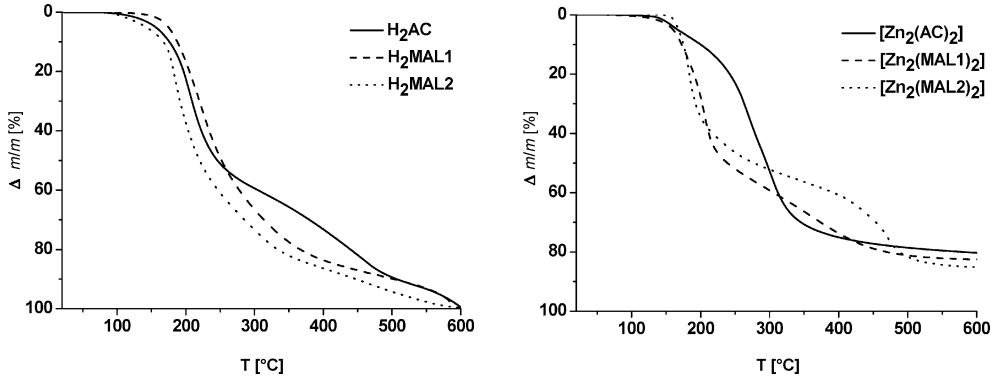

Figure 6. Curve for the weight loss of H_2L and the Zn complexes under nitrogen.

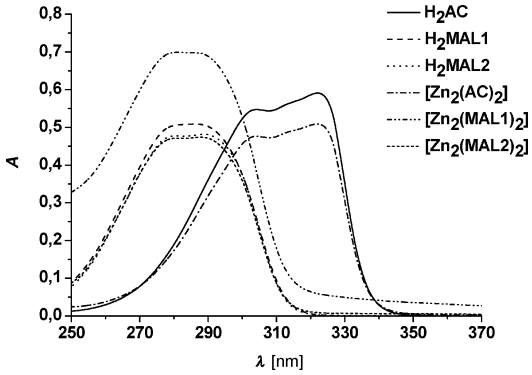

Figure 7. Absorption spectra of H_2L and the Zn complexes in methanol ($C = 10^{-6}$ M).

The main absorption bands for H_2AC are located at 305 nm ($\log\varepsilon = 5.74$) and 321 nm ($\log\varepsilon = 5.77$) and can be attributed to the electronic transitions within the rings formed by intramolecular hydrogen bonds.[21] The variation of R from $–CH_3$ (H_2AC) to $–OCH_3$ (H_2MAL1) and $–OC(CH_3)_3$ (H_2MAL2) (Figure 1) leads to a hypsochromic shift (≈ 30 nm) of the maxima, while the absorption coefficients remain in the same range ($\log\varepsilon \approx 5.68–5.71$). Ueno and Martell[21] have explained the shift by the –I effect of the substituents; in our case $–OCH_3$ and $–OC(CH_3)_3$ lead to the keto–enamine form as the major species for H_2MAL1 and H_2MAL2 [Figure 2, form (3)]. The absorption bands of the zinc complexes show no observable shift with respect to the free ligands and remain almost as intense ($\log\varepsilon \approx 5.68–5.84$). The combination of the spectrophotometric titration (see an example for the zinc complex with H_2AC: Figures S1 and S2, Table S2) and the ESI-MS characterization suggests the existence of at least the mononuclear [ZnL] species in methanol solution.

Emission Spectra

The emission spectra of H_2L and Zn_2L_2 were measured for the solid-state samples only at 77 K because of the low luminescence of these compounds. Under excitation at 337 nm, the luminescence spectra of the Schiff bases and their zinc complexes exhibit broad bands with maxima located in the blue (Figure 8, Table 3). The electronic effects generated by the substituents R have the same influence on the emission spectra as that on the absorption spectra: a hypsochromic shift of the emission maxima in going from H_2AC to H_2MAL1 and H_2MAL2. By comparing the emission spectra of the zinc complexes with those of the free Schiff bases, one can note: (i) for the couple $[Zn_2(AC)_2]$/H_2AC, a small redshift (≈10 nm) in the emission maximum with an increase in intensity of the shoulder at ≈ 520 nm, (ii) for the couple $[Zn_2(MAL1)_2]$/H_2MAL1, a small blueshift (≈10 nm) in the emission maximum with the almost complete disappearance of the shoulder at 530 nm, and (iii) for the couple $[Zn_2(MAL2)_2]$/H_2MAL2, a small blueshift of the emission band. The highest luminescence quantum yield among the compounds studied is observed for $[Zn_2(MAL1)_2]$ (Table 3). Unfortunately, the low emission quantum yields prevented a deeper analysis of the optical properties of these compounds.

Table 3. Relative quantum yields and emission maxima for H_2L and the Zn complexes at 77 K.

Compound	λ [nm][a]	$Q_{rel.}$ [a.u.]
H_2AC	450 sh., *475*, 520 sh.	0.4
H_2MAL1	*415*, 455 sh.	0.5
H_2MAL2	*425–475*	0.3
$[Zn_2(AC)_2]$	430 sh., *464*, 525 sh.	0.1
$[Zn_2(MAL1)_2]$	*425*, 462, 530 sh.	1.0
$[Zn_2(MAL2)_2]$	*430–490*, 530 sh.	0.2

[a] Maxima of the emission bands are in *italic*.

Conclusions

In this paper, we propose the use of a convenient synthetic route for the isolation of pure helical Zn_2L_2 species in a high yield,[14] thanks to the high reactivity of $Zn(Et)_2$ with Schiff bases having a strong acidic character. Moreover, these organic ligands, derivatives of β-diketones or β-keto esters and ethylenediamine, possess sufficient flexibility that allows their wrapping around the metal ions with the formation of double-stranded, helical, dinuclear species, which is most favorable for a tetrahedral coordination envi-

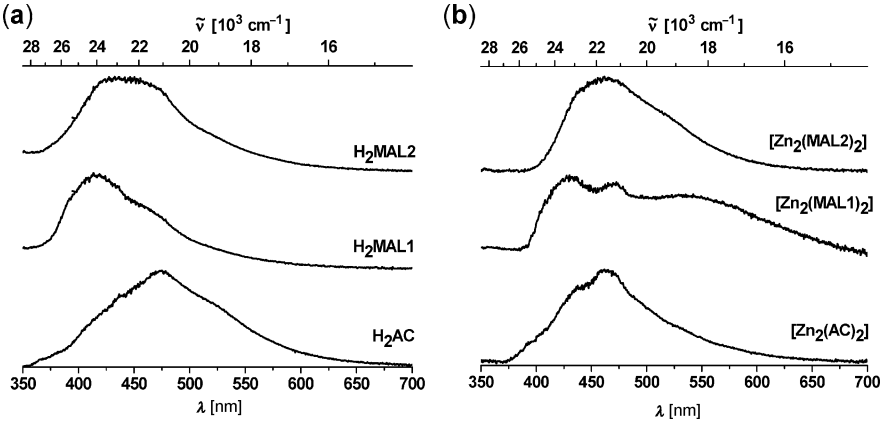

Figure 8. Luminescence spectra of H_2L and the Zn complexes upon excitation at 337 nm; $T = 77$ K.

ronment such as that of Zn. Besides the possible application of zinc Schiff bases complexes as fluorescent materials,[2–6] there is also the possibility of using such compounds as precursors for the development of porous structures with well-defined interfaces for storage of different gases (CH_4, CO_2, etc.),[22] as well as for the nano- and microfabrication of zinc oxide materials.[23] In view of the latter application, the low stability of the zinc complexes studied (≈150–160 °C) could be an advantage. Finally, the helicity of the Zn_2L_2 complexes is of utmost importance for the design of entangled structures such as knotanes.[24]

Experimental Section

Materials and General Methods

Commercially available ethylenediamine ($C_2H_8N_2$, Aldrich), acetylacetone ($C_5H_8O_2$, Hacac, Aldrich), methylacetoacetate ($C_5H_8O_3$, Hmaoac, Aldrich), *tert*-butylacetoacetate ($C_8H_{14}O_2$, Htbaoac, Aldrich), and zinc acetate dihydrate ($ZnC_4H_{10}O_6$, Aldrich), as well as solvents such as benzene (Aldrich, 99.8%) and toluene (Aldrich, 99.8%) were used without further purification. $CDCl_3$ (99.8 at.-% D, Aldrich) was utilized for the ^1H NMR spectra determination. Elemental analyses (C, H, N) were performed by the Microanalytical Service of the Center for Drug Chemistry (Moscow, Russia). IR spectra were recorded in the range 4000–600 cm^{-1} by using a Perkin–Elmer Spectrum One spectrometer equipped with a universal attenuated total reflection sampler. ^1H NMR spectra were measured on an Avance-400 (Bruker, 400 MHz) spectrometer. Thermogravimetric analysis was performed on a Q–1500 thermal analyzer under nitrogen at a heating rate of 5 °C min^{-1}. UV/Vis absorption spectra of the solutions and reflectance spectra of the solid-state samples of the Schiff bases and zinc complexes as well as spectrophotometric titrations were recorded on a Lambda 35 spectrophotometer (Perkin–Elmer). The composition of the zinc complexes in methanol solution was determined by using the Method of Continuous Variation. All titrations were performed in a thermostatted (25.0 ± 1 °C) glass-jacketed vessel at $I = 0.01$ (tetrabutylammonium perchlorate, Acros). ESI-MS spectra were obtained by using an Agilent LC/MSD 1100SL spectrometer with 5×10^{-3} M solutions of $Zn(CH_3COO)_2 \cdot 2H_2O$ and H_2L in methanol, and a capillary temperature of 120 °C. Direct infusion of the analyzed solution was used. The optimum flow rate was 12 μL min^{-1}. The capillary exit was maintained at a potential of 3.5–5.5 keV. All analyses were conducted in positive mode. Luminescence spectra of the solid-state samples were measured at 77 K on a multichannel spectrometer S2000 (Ocean Optics), which utilizes a nitrogen laser LGI-21 (λ_{ex} = 337 nm) as an excitation source. The spectra were corrected for the instrumental functions. Relative quantum yields were calculated with the following Equation (2).

$$Q_{rel} = \frac{Q_x}{Q_r} = \left(\frac{1-R_r}{1-R_x}\right)\left(\frac{\varphi_x}{\varphi_r}\right) \quad (2)$$

where Q is the quantum yield, R is the amount of reflected excitation radiation, and ϕ is the integrated area of the corrected luminescence spectra. $Zn_2(MAL1)_2$ was considered as a reference and for the sake of comparison its quantum yield was set to 1. Each sample was measured at least three times. The estimated error for the luminescence relative quantum yields is ±15%.

Synthesis of the Schiff Bases (H_2L): The Schiff bases were prepared according to the literature procedure.[25] Ethylenediamine (0.3 mL, 1 mmol) was added to acetylacetone (0.9 mL, 2 mmol) for H_2AC, to methylacetoacetate (1.0 mL, 2 mmol) for H_2MAL1, or to *tert*-butylacetoacetate (0.8 mL, 2 mmol) for H_2MAL2, dissolved in benzene (20 mL). The resulting white precipitates were filtered off and dried for 30 min at 80 °C and $P = 10^{-2}$ Torr.

H_2AC – *N,N′*-Ethylene-bis(4-iminopentan-2-one): Yield: 0.213 g (95%). $C_{12}H_{20}N_2O_2$ (224.30): calcd. C 64.3, H 8.9, N 12.5; found C 64.0, H 9.1, N 12.5. IR (Diamond ATR): ν(C–H) + ν(N–H) = 3306, 3162, 3070, 2988, 2958, 2916; ν(C=C) + ν(C=N) + ν(C=O) = 1614, 1568, 1542; δ(O–H) = 1378, 1352, 1384, 1326, 1276; ν(C–O–H) = 1194, 1088, 1022 cm^{-1}. ^1H NMR (400 MHz, $CDCl_3$/TMS, 25 °C): δ = 10.88 (s, 2 H, –OH), 4.98 (s, 2 H, –CH–), 3.41 (t, $^3J_{H,H}$ = 6.4 Hz, 4 H, $–CH_2–$), 1.98 (d, $^3J_{H,H}$ = 4.0 Hz, 6 H, $–CH_3$), 1.89 (d, $^3J_{H,H}$ = 4.0 Hz, 6 H, $–CH_3$) ppm.

H_2MAL1 – *N,N′*-Ethylene-bis(methyl-3-iminobutanoate): Yield: 0.243 g (95%). $C_{12}H_{20}N_2O_4$ (256.30): calcd. C 56.2, H 7.9, N 12.9; found C 56.1, H 7.9, N 13.1. IR (Diamond ATR): ν(C–H) + ν(N–H) = 3306, 3162, 3006, 2834; ν(C=C) + ν(C=N) + ν(C=O) = 1656, 1582; δ(O–H) = 1374, 1352, 1278; ν(C–O–H) + ν(C–O–C) = 1170, 1096, 1058, 1036, 1002 cm^{-1}. ^1H NMR (400 MHz, $CDCl_3$/TMS): δ = 8.64 (s, 2 H, –OH), 4.50 (s, 2 H,–CH–), 3.62 (s, 6 H,$–OCH_3$), 3.38 (t, $^3J_{H,H}$ = 4.0 Hz, 4 H, $–CH_2–$), 1.92 (s, 6 H, $–CH_3$) ppm.

H_2MAL2 – *N,N′*-Ethylene-bis(*tert*-butyl-3-iminobutanoate): Yield: 0.323 g (95%). $C_{18}H_{32}N_2O_4$ (340.46): calcd. C 63.5, H 9.4, N 8.2; found C 62.8, H 9.9, N 8.1. IR (Diamond ATR): ν(C–H) + ν(N–H) = 3268, 3182, 2970, 2928; ν(C=C) + ν(C=N) + ν(C=O) = 1642, 1606; δ(O–H) = 1390, 1364, 1288; ν(C–O–H) + ν(C–O–C) = 1150, 1102, 1046 cm^{-1}. ^1H NMR (400 MHz, $CDCl_3$/TMS): δ = 8.61 (s, 2 H, –OH), 4.43 (s, 2 H, –CH–), 3.35 (d, $^3J_{H,H}$ = 4.0 Hz, 4 H, $–CH_2–$), 1.89 (s, 6 H, $–CH_3$), 1.47 [d, 18 H, $–C(CH_3)_3$] ppm.

Table 4. Crystal data and structure refinement parameters for H_2MAL1 (**1**) and H_2MAL2 (**2**).

	1	**2**
Formula unit	$C_{12}H_{20}N_2O_4$	$C_{18}H_{32}N_2O_4$
Molecular weight	256.30	340.46
T [K]	183(2)	120(2)
Crystal system	monoclinic	triclinic
Space group	$C2/c$	$P\bar{1}$
$Z(Z')$	4(0.5)	2(1)
a [Å]	19.401(4)	9.522(4)
b [Å]	5.455(1)	9.920(4)
c [Å]	13.067(3)	11.114(4)
α [°]	90	91.223(9)
β [°]	111.62(3)	111.002(8)
γ [°]	90	90.699(9)
V [Å^3]	1285.6(4)	979.7(7)
$\rho_{calcd.}$ [g cm^{-3}]	1.324	1.154
μ [cm^{-1}]	0.99	0.81
$F(000)$	552	372
$2\theta_{max}$ [°]	63	52
Reflections measured (R_{int})	3189 (0.063)	5087
Independent reflections	3120	3670
Observed reflections [$I > 2\sigma(I)$]	1417	1754
Number of parameters	122	233
Final R (F_{hkl})	0.1713	0.1396
ωR_2	0.1104	0.1809
GOF	0.907	1.049
R_1 [$I > 2\sigma(I)$]	0.0461	0.0786
Δg_{max}, Δg_{min} [e Å^{-3}]	0.412, –0.214	0.370, –0.331

Table 5. Crystal data and structure refinement parameters for $[Zn_2(AC)_2]\cdot C_6H_6$ (**3**), $[Zn_2(MAL1)_2]\cdot 0.5C_7H_8$ (**4**), and $[Zn_2(MAL2)_2]\cdot C_7H_8$ (**5**).

	3	**4**	**5**
Formula unit	$C_{30}H_{42}N_4O_4Zn_2$	$C_{27.5}H_{40}N_4O_8Zn_2$	$C_{43}H_{68}N_4O_8Zn_2$
Molecular weight	653.45	684.8	899.79
T [K]	150(2)	150(2)	150(2)
Crystal system	monoclinic	triclinic	monoclinic
Space group	$C2/c$	$P\bar{1}$	$C2/c$
$Z(Z')$	4(0.5)	2(2)	4(0.5)
a [Å]	12.514(4)	12.801(3)	21.166(4)
b [Å]	16.819(6)	15.151(3)	10.275(2)
c [Å]	14.557(6)	16.343(3)	23.171(5)
α [°]	90	102.59(3)	90
β [°]	103.27(3)	94.64(3)	114.64(3)
γ [°]	90	95.30(3)	90
V [Å^3]	2982.1(2)	3063.6(1)	4580.4(2)
$\rho_{calcd.}$ [g cm^{-3}]	1.455	1.412	1.328
μ [cm^{-1}]	16.50	16.19	11.10
$F(000)$	1368	1428	1904
$2\theta_{max}$ [°]	60	56	56
Reflections measured (R_{int})	18691	27879	18688
Independent reflections	4468	13625	5252
Observed reflections [$I > 2\sigma(I)$]	4095	8668	3829
Number of parameters	185	748	271
Final R (F_{hkl})	0.0313	0.0884	0.0619
ωR_2	0.0614	0.1490	0.1049
GOF	1.129	0.890	0.903
R_1 [$I > 2\sigma(I)$]	0.0271	0.0558	0.0406
Δg_{max}, Δg_{min} [e Å^{-3}]	0.429, –0.380	0.706, –1.802	0.887, –0.587

Synthesis of the Zn Complexes (Zn_2L_2): The zinc complexes were synthesized according to the synthetic method described in the literature.[14] These reactions were carried out under a dry nitrogen atmosphere by using Schlenk techniques. Diethylzinc [$Zn(Et)_2$, 1 mmol] was added to the corresponding Schiff base (H_2L, 1 mmol) in benzene for H_2AC or toluene for H_2MAL1 and H_2MAL2. The solutions were then cooled to ≈5 °C, and the precipitated crystals were filtered off and dried for 1 h at 90 °C and under a pressure of 10^{-2} Torr.

$Zn_2(AC)_2$ – Bis[*N*,*N*′-ethylene-bis(4-iminopentan-2-ono)]zinc: Yield: 0.518 g (90%). $Zn_2(C_{12}H_{18}N_2O_2)_2$ (575.33): calcd. C 51.6, H 6.9, N 10.6; found C 51.1, H 6.5, N 10.3. IR: ν(C–H) = 3060, 2990, 2956, 2916, 2850; ν(C=C) + ν(C=N) + ν(C=O) = 1610, 1580 cm^{-1}. ^{1}H NMR (400 MHz, $CDCl_3$/TMS): δ = 4.93 (s, 4 H, –CH–), 3.29 (s, 8 H, –CH_2–), 1.79 (s, 6 H, –CH_3), 1.73 (s, 6 H, –CH_3) ppm. ESI-MS (EI$^+$): m/z (%) = 286.9 (80) [Zn(AC)+H$^+$]$^+$.

$Zn_2(MAL1)_2$ – Bis[*N*,*N*′-ethylene-bis(methy-3-iminobutanoato)]zinc: Yield: 0.549 g (86%). $Zn_2(C_{12}H_{18}N_2O_4)_2$ (639.33): calcd. C 45.1, H 5.7, N 8.8; found C 45.1, H 6.1, N 8.5. IR: ν(C–H) = 3008, 2959; ν(C=C) + ν(C=N) + ν(C=O) = 1655, 1582; ν(CH_3–O) = 1098, 1060 cm^{-1}. ^{1}H NMR (400 MHz, $CDCl_3$/TMS): δ = 4.50 (s, 4 H, –CH–), 3.62 (s, 12 H, –OCH_3), 3.37 (t, $^3J_{H,H}$ = 4.0 Hz, 8 H, –CH_2–), 1.92 (s, 12 H, –CH_3) ppm. ESI-MS (EI$^+$): m/z (%) = 305.0 (25) [Zn(MAL1) – CH_3+H$^+$]$^+$, 319.0 (100) [Zn(MAL1)+H$^+$]$^+$.

$Zn_2(MAL2)_2$ – Bis[*N*,*N*′-ethylene-bis(*tert*-butyl-3-iminobutanoato)]-zinc: Yield: 0.743 g (92%). $Zn_2(C_{18}H_{30}N_2O_4)_2$ (807.65): calcd. C 53.5, H 7.5, N 6.9; found C 53.3, H 7.5, N 6.7. IR: ν(C–H) = 2970, 2927; ν(C=C) + ν(C=N) + ν(C=O) = 1642, 1604; ν[$(CH_3)_3$C–O] = 843, 833, 815 cm^{-1}. ^{1}H NMR (400 MHz, $CDCl_3$/TMS): δ = 4.41 (s, 4 H, –CH–), 3.34 (t, $^3J_{H,H}$ = 4.0 Hz, 8 H, –CH_2–), 1.87 (s, 12 H, –CH_3), 1.45 [s, 36 H, –$OC(CH_3)_3$] ppm. ESI-MS (EI$^+$): 347.0 (100) [Zn(MAL2) – $C(CH_3)_3$+H$^+$]$^+$, 403.0 (50) [Zn(MAL2)+H$^+$]$^+$.

X-ray Diffraction Analysis: Single crystals of H_2MAL1 (**1**) and H_2MAL2 (**2**) suitable for X-ray analysis were obtained by slow evaporation of benzene solutions. The single crystals of $[Zn_2(AC)_2]\cdot C_6H_6$ (**3**) were obtained by slow evaporation of a benzene solution covered by a thin layer of pentane, while those of $[Zn_2(MAL1)_2]\cdot 0.5C_7H_8$ (**4**) and $[Zn_2(MAL2)_2]\cdot C_7H_8$ (**5**) were simply formed by cooling down of the toluene solution.

X-ray diffraction analysis was carried out with: a Syntex $P2_1$ (Mo-K_α-radiation, λ = 0.71073 Å) at 183 K for H_2MAL1 (**1**), a SMART 1000 CCD (Mo-K_α-radiation, λ = 0.71073 Å) at 120 K for H_2MAL2 (**2**), and an automatic diffractometer IPDS (Stoe) (Mo-K_α-radiation, λ = 0.71073 Å) with Imaging Plate detector at 150 K for $[Zn_2(AC)_2]\cdot C_6H_6$ (**3**), $[Zn_2(MAL1)_2]\cdot 0.5C_7H_8$ (**4**), and $[Zn_2(MAL2)_2]\cdot C_7H_8$ (**5**). Details of the data collection and structure refinement for the Schiff bases are presented in Table 4, while those for the Zn complexes are listed in Table 5. CCDC-722310 (for **1**), -722309 (for **2**), -722311 (for **3**), -722312 (for **4**), and -722313 (for **5**) contain the supplementary crystallographic data for this paper. These data can be obtained free of charge from The Cambridge Crystallographic Data Centre via www.ccdc.cam.ac.uk/data_requiest.cif.

Supporting Information (see footnote on the first page of this article): Tables gathering the thermal stability data (for H_2L and their zinc complexes) as well as the spetrophotometric titration of ligand H_2AC with Zn.

Acknowledgments

This work was supported through grants from the Russian Foundation for Basic Research (No. 07-02-00495, 06-02-16399, 09-03-00850) as well as by the Development Program of Leading Scientific Schools in Russia (No. NH-4365.2008.2). We also thank A.

Borisenko, S. Kardashev, O. Boytsova, I. Docenko, I. Kolesnik, T. Shatalova, and L. Lepnev for their assistance in the characterization of the compounds.

[1] a) D. J. Darensbourg, *Chem. Rev.* **2007**, *107*, 2388–2410; b) S. J. Wezenberg, A. W. Kleij, *Angew. Chem. Int. Ed.* **2008**, *47*, 2354–2364; c) L. San Felices, E. C. Escudero-Adán, J. Benet-Buchholz, A. W. Kleij, *Inorg. Chem.* **2009**, *48*, 846–853; d) A. W. Kleij, *Chem. Eur. J.* **2008**, *14*, 10520–10529; e) S. Alkine, S. Kagiyama, T. Nabeshima, *Inorg. Chem.* **2007**, *46*, 9525–9527; f) S. Akine, S. Sunaga, T. Taniguchi, H. Miyazaki, T. Nabeshima, *Inorg. Chem.* **2007**, *46*, 2959–2961; g) S. J. Wezenberg, E. C. Escudero-Adán, J. Benet-Buchholz, A. W. Kleij, *Inorg. Chem.* **2008**, *47*, 2925–2927.

[2] a) D. C. Freeman, C. E. White, *J. Am. Chem. Soc.* **1956**, *78*, 2678–2682; b) C. E. White, F. Cuttitta, *Anal. Chem.* **1959**, *31*, 2083–2087; c) R. M. Dagnall, R. Smith, T. S. West, *J. Chem. Soc. A* **1966**, 1595–1598; d) G. Yu, S. Yin, Y. Liu, Z. Shuai, D. Zhu, *J. Am. Chem. Soc.* **2003**, *125*, 14816–14824.

[3] a) J. Zhang, S. Gao, C.-M. Che, *Eur. J. Inorg. Chem.* **2004**, 956–959; b) L. S. Sapochak, F. E. Benincasa, R. S. Schofield, J. L. Baker, K. K. C. Riccio, D. Fogarty, H. Kohlemann, K. F. Ferris, P. E. Burrows, *J. Am. Chem. Soc.* **2002**, *124*, 6119–6125; c) X. Chen, Q. Zhou, Y. Cheng, Y. Geng, D. Ma, Z. Xie, L. Wang, *J. Lumin.* **2007**, *126*, 81–90.

[4] a) C. Wang, Z. Yang, Y. Li, Z. Yang, Y. Li, L. Gong, G. Zhao, *Phys. Status Solidi* **2002**, *191*, 117–124; b) A. V. Metelitsa, A. S. Burlov, S. O. Bezuglyi, I. G. Borodkina, V. A. Bren′, A. D. Garnovskii, V. I. Minkin, *Russ. J. Coord. Chem.* **2006**, *32*, 858–869; c) Y. Hamada, T. Sano, M. Fujita, T. Fujii, Y. Nishio, K. Shibata, *Jpn. J. Appl. Phys.* **1993**, *32*, L511–L513; d) G. Yu, Y. Liu, Y. Song, X. Wu, D. Zhu, *Synth. Met.* **2001**, *117*, 211–214; e) M. G. Kaplunov, S. S. Krasnikova, I. K. Yakushenko, S. N. Shamaev, A. P. Pivovarov, O. N. Efimov, *Mol. Cryst. Liq. Cryst.* **2005**, *426*, 287–293; f) P. Wang, Z. Hong, Z. Xie, S. Tong, O. Wong, C.-S. Lee, N. Wong, L. Hung, S. Lee, *Chem. Commun.* **2003**, 1664–1665; g) S. Tokito, K. Noda, H. Tanaka, Y. Taga, T. Tsutsui, *Synth. Met.* **2000**, *111–112*, 393–396; h) T. Sano, Y. Nishio, Y. Hamada, H. Takahashi, T. Usuki, K. Shibata, *J. Mater. Chem.* **2000**, *10*, 157–161; i) S. P. Singh, Y. N. Mohapatra, M. Qureshi, S. Sundar Manoharan, *Synth. Met.* **2005**, *155*, 376–379; j) X. Xu, Y. Liao, G. Yu, H. You, C. Di, Z. Su, D. Ma, Q. Wang, S. Li, S. Wang, J. Ye, Y. Liu, *Chem. Mater.* **2007**, *19*, 1740–1748.

[5] J. K.-H. Hui, Z. Yu, M. J. MacLachlan, *Angew. Chem. Int. Ed.* **2007**, *46*, 7980–7983.

[6] a) M. E. Germain, T. R. Vargo, P. G. Khalifan, M. J. Knapp, *Inorg. Chem.* **2007**, *46*, 4422–4429; b) M. E. Germain, T. R. Vargo, B. A. McClure, J. J. Rack, P. G. Van Patten, M. Odol, M. J. Knapp, *Inorg. Chem.* **2008**, *47*, 6203–6211; c) E. M. E. Germain, M. J. Knapp, *J. Am. Chem. Soc.* **2008**, *130*, 5422–5423.

[7] a) G. E. Batley, D. P. Graddon, *Aust. J. Chem.* **1967**, *20*, 877–883; b) G. E. Batley, D. P. Graddon, *Aust. J. Chem.* **1967**, *20*, 885–891.

[8] D. Hall, F. H. Moore, *J. Chem. Soc. A* **1966**, 1822–1824.

[9] a) J. Reglinski, S. Morris, D. E. Stevenson, *Polyhedron* **2002**, *21*, 2175–2182; b) S. Mizukami, H. Houjou, Y. Nagawa, M. Kanesato, *Chem. Commun.* **2003**, 1148–1149; c) S. Mizukami, H. Houjou, K. Sugaya, E. Koyama, H. Tokuhisa, T. Sasaki, M. Kanesato, *Chem. Mater.* **2005**, *17*, 50–56.

[10] a) Z. Wu, Q. Chen, S. Xiong, B. Xin, Z. Zhao, L. Jiang, J. S. Ma, *Angew. Chem. Int. Ed.* **2003**, *42*, 3271–3274; b) A. M. García-Deibe, J. Sanmartín Matalobos, M. Fondo, M. Vázquez, M. R. Bermejo, *Inorg. Chim. Acta* **2004**, *357*, 2561–2569; c) R. Pedrido, M. R. Bermejo, M. J. Romero, A. M. González-Noya, M. Manerio, M. I. Fernández, *Inorg. Chem. Commun.* **2005**, *8*, 1036–1040; d) M. Böring, S. Link, C. D. Brandt, E. C. Tejero, *Eur. J. Inorg. Chem.* **2007**, 1661–1670; e) A. D. Wang, C. F. Bi, Y. H. Zou, J. K. Xu, Y. H. Kan, *Russ. J. Coord. Chem.* **2008**, *34*, 475–479; f) M. Isola, F. Balzano, V. Liuzzo, F. Marchetti, A. Raffaelli, G. Uccello Barretta, *Eur. J. Inorg. Chem.* **2008**, 1363–1375.

[11] P. G. Cozzi, *Chem. Soc. Rev.* **2004**, *33*, 410–421.

[12] G. E. Bately, D. P. Graddon, *Aust. J. Chem.* **1967**, *20*, 885–891.

[13] M. J. O'Connor, B. O. West, *Aust. J. Chem.* **1967**, *20*, 2077–2085.

[14] G. A. Morris, H. Zhou, C. L. Stern, S. T. Nguyen, *Inorg. Chem.* **2001**, *40*, 3222–3227.

[15] N. Bresciani-Pahor, M. Calligaris, G. Nordin, L. Randaccio, *Acta Crystallogr., Sect. B* **1979**, *35*, 2776–2778.

[16] Z.-M. Jin, M.-C. Li, M.-L. Hu, M.-L. Hu, L. Shen, *Acta Crystallogr., Sect. C* **2004**, *60*, o642–o643.

[17] a) S. Floquet, N. Ouali, B. Bocquet, G. Bernardinelli, D. Imbert, J.-C. G. Bünzli, G. Hopfgartner, C. Piguet, *Chem. Eur. J.* **2003**, *9*, 1860–1875; b) S. N. Semenov, A. Yu. Rogachev, S. V. Eliseeva, C. Pettinari, F. Marchetti, A. A. Drozdov, S. I. Troyanov, *Chem. Commun.* **2008**, 1992–1994; c) S. D. Reid, A. J. Blake, C. Wilson, J. B. Love, *Inorg. Chem.* **2006**, *45*, 636–643.

[18] S. Wang, *Coord. Chem. Rev.* **2001**, *215*, 79–98.

[19] A. de Bettencourt-Dias, *Dalton Trans.* **2007**, 2229–2241.

[20] R. C. Evans, P. Douglas, C. J. Winscom, *Coord. Chem. Rev.* **2006**, *250*, 2093–2126.

[21] K. Ueno, A. E. Martell, *J. Phys. Chem.* **1957**, *61*, 257–261.

[22] a) O. M. Yaghi, M. O'Keeffe, N. W. Ockwig, H. K. Chae, M. Eddaoudi, J. Kim, *Nature* **2003**, *423*, 705–714; b) M. Eddaoudi, J. Kim, N. Rosi, D. Vodak, J. Wachter, M. O'Keeffe, O. M. Yaghi, *Science* **2002**, *295*, 469–472; c) A. K. Cheetham, C. N. R. Rao, R. K. Feeler, *Chem. Commun.* **2006**, 4780–4795; d) B. Wang, A. P. Côté, H. Fukukawa, M. O'Keefe, O. M. Yaghi, *Nature* **2008**, *453*, 207–211.

[23] a) S. Jung, W. Cho, H. J. Lee, M. Oh, *Angew. Chem. Int. Ed.* **2009**, *48*, 2–6; b) X. Liu, *Angew. Chem. Int. Ed.* **2009**, *48*, 2–6.

[24] O. Lukin, F. Vögtle, *Angew. Chem. Int. Ed.* **2005**, *44*, 1456–1477.

[25] H. Schiff, *Justus Liebigs Ann. Chem.* **1864**, *131*, 118–119.

Received: April 1, 2009
Published Online: July 6, 2009

